S.R. Chalov[1], A.S. Tsyplenkov[2]

[1] M.V. Lomonosov Moscow State University, Faculty of Geography, Land Hydrology Department, e-mail: srchalov@geogr.msu.ru

[2] M.V. Lomonosov Moscow State University, Geography Department, N.I.Makkaveev Scientific Research Laboratory for Soils Erosion and Fluvial Processes, e-mail: atsyplenkov@geogr.msu.ru

Short-term dynamics of river water turbidity

Abstract: An overview of the recently collected datasets of highly discrete water turbidity measurements has allowed for the first hydrological and geographical analysis of short-term fluctuations in water turbidity and the composition of suspended sediments. The novel methodology has been developed to estimate a value of TI, which is the ratio of the difference between the maximum and minimum turbidity for a short period of time (ΔTi) (1 hour with the measurement frequency of 20 minutes) and the total turbidity difference for the water regime phase under study (ΔT_{HE}). Higher TI values correspond to a greater contribution of diurnal (20-minute) turbidity fluctuations to the seasonal variability of sediment yield. Rivers have been grouped according to the value of water turbidity fluctuations within one hour (20-minute): glacier-fed rivers (the Tarfala, the Dzhankuat) (TI amounts to 0.17-0.22); volcanic rivers (0.22–0.25) and lowland rivers (the Selenga, the Western Dvina) (0.09).

Keywords: river flow, sediment concentrations, short-term changes

1. Introduction

One of the characteristics of a river sediment load is the turbidity of water (S), which is indicative of the content of suspended particles in water and is measured in terms of the substance content ($g \cdot m^{-3}$, $mg \cdot l^{-1}$) (Karaushev Ed., 1977). The most common worldwide indirect method of measuring the water turbidity is the optical (photometric, nephelometric) analysis (Gray and Gartner, 2009; Lewis, 1996; Walling, 1977), which allows the determination of optical turbidity (T). The main objective was to measure the optical density of a sample and the ability of suspended particles to scatter light (Belozerova and Chalov, 2013). Scattering and absorption of light occur not only on mineral but also on organic suspended particles, air bubbles and other irregularities in a sample of water (Gippel, 1995), which, in turn, affects the results of optical turbidity measurement. Such errors can cause a second variation of turbidity (Clifford et al., 1995) Valais, Switzerland. The data include hourly pump-sampler suspended sediment data from June to September 1990; a quasi-continuous 24 hour record of turbidity

and velocity sampled at 5 second intervals in July 1992; and 3-minute series of turbidity and velocity at various heights in the boundary layer sampled at 10Hz, also obtained in July 1992. The high-frequency measurements made in 1992 employed an active head, infrared suspended solids monitor deployed in close proximity to a twin-axis, discoidal electromagnetic current meter. Data were analysed using a combination of statistical and deterministic (\u2018event structure\u2019.

A more significant contribution is made by fluctuations caused by the dynamics of turbulent formations, which were first theoretically described by A.V. Karaushev (1977). At the same time, turbidity fluctuations caused by turbulence occur on a scale of 10-20 sec and cause fluctuations of up to 1% of the total sediment load during the season (Clifford et al., 1995)Valais, Switzerland. The data include hourly pump-sampler suspended sediment data from June to September 1990; a quasi-continuous 24 hour record of turbidity and velocity sampled at 5 second intervals in July 1992; and 3-minute series of

turbidity and velocity at various heights in the boundary layer sampled at 10 Hz, also obtained in July 1992. The high-frequency measurements made in 1992 employed an active head, infrared suspended solids monitor deployed in close proximity to a twin-axis, discoidal electromagnetic current meter. Data were analysed using a combination of statistical and deterministic ('event structure'. A much more significant contribution is made by 30-minute (up to 10%) and diurnal (up to 30%) turbidity fluctuations. This is supported by the results of research on the US rivers (Horowitz et al., 1990), showing that significant turbidity fluctuations occur within 20-30 minutes.

The implementation of high-precision digital recording instruments increased the effi-

ciency, completeness as well as the spatial and temporal resolution of water flow and sediment load observation data. The analysis of turbidity data received from high-frequency self-recording devices is widely covered by scientists, with special attention paid to the investigation of rivers in periglacial conditions (Stott and Grove, 2001; Stott and Mount, 2007a; Stott and Mount, 2007b) but does not examine processes explicitly linked to the periglacial environment. Three glacierized basins were studied: Austre Brøggerbreen and Midre Lov´ enbreen, Svalbard (79°N, 12 °E. Nevertheless, the patterns of highly discrete turbidity fluctuations remain poorly studied at specific reaches of rivers (Alekseevskiy et al., 2013).

2. Materials and Methods

During field studies carried out by the Moscow State University, Faculty of Geography in 2012-2017, datasets on water turbidity and stages using

self-recording devices were obtained on 9 rivers (Fig. 1). Within the framework of this study, high-frequency data were analysed, obtained

Figure 1. The surveyed rivers: 1 – the Khaara river; 2 – the Selenga river; 3,4 – the Sukhaya Elizovskaya; 5 – the Tarfala river; 6 – the Tsanyk river; 7 – the Langeri river; 8 – the Dzhankuat river; 9 – the Sukhoy Ilchinets river; 10 – the Velesa river; 11,12 – the Tarfala river

from 12 self-recording devices (loggers) on the level (H) and optical turbidity of water (T, NTU). The devices were installed in rivers located in different natural conditions. The datasets cover different periods (from 2 to 149 days) and were recorded with different frequencies (from 2 to 15 min; see Table 1). To avoid turbulent and instrumental errors, as well as to standardize the measurements, all data were averaged to a 20-minute interval of observations.

Table 1. Available turbidity (T, NTU) datasets used in the study

Logger model	River	Station location	Station code	Beginning	End	Period, days	Measurement frequency, min
YSI 6820 V2	Khaara	Small plain river, near Buren Tolgoy	1	06.05.12	03.09.12	121	15
SEBA MPS-D8/ Qualilog8	Selenga	Large river below Ulan-Ude	2	15.06.12	30.06.12	6	2
SEBA MPS-D8/ Qualilog8	Sukhaya Yelizovskaya	Lakhar valley, middle reach	3	30.07.12	01.08.12	2	2
SEBA MPS-D8/ Qualilog8	Sukhaya Yelizovskaya	Mountain, the upper reach	4	19.06.14	21.06.14	2	2
LISST	Tarfala	Small mountain river below glacier	5	22.07.14	25.07.14	3	2
SEBA MPS-D8/ Qualilog8	Tsanyk	Small mountain river	6	09.04.15	12.04.15	3	2
SEBA MPS-D8/ Qualilog8	Langery	Mountain small river below placer mining	7	01.06.15	20.08.15	80	2
ANALITE NEP495	Dzhankuat	Mountain river below glacier	8	15.06.16	20.07.16	35	15
ANALITE NEP495	Sukhoy Ilchinets	Small mountain river	9	14.08.16	23.08.16	9	1
RBR SOLO Tu	Velesa	Small plain river	10	27.05.17	23.10.17	149	5
ANALITE NEP495	Tarfala	Mountain river mouth	11	11.08.17	25.08.17	14	10
SEBA MPS-D8/ Qualilog8	Tarfala	Mountain river below glacier	12	15.08.17	27.08.17	12	10

River hydrographs were divided into separate hydrological events, within which further analysis was performed. To separate the flow events from the base flow periods of the river hydrographs, the local-minimum method was used. This method determines the base flow by linking the minimum flow between the events (Sloto and Crouse, 1996) sliding-interval, and local-minimum methods. The program also describes the frequency and duration of measured streamflow and computed base flow and surface runoff. Daily mean stream discharge is used as input to the program in either an American Standard Code for Information Interchange (ASCII, which is a mathematical interpretation of the graphical method of B.V. Polyakov (1946). The local minimum method verifies each value to determine whether it is the lowest level per one half of the interval minus 1 time unit before and after the considered one. If so, then it is a local minimum. A hydrological event will be the change in water runoff over a period of time between adjacent local minima (Fig. 2). A total of 197 hydrological events were identified, with an average duration of 39 hours (Table 2).

Table 2. Analysed hydrological events

River	Station code[1]	Number of HE	Duration, hours	T_{AV}, NTU	ΔT, NTU
Khaara	1	74	44.5 ± 37.5	172	1 128
Selenga	2	2	2.3 ± 0.3	221	622
Sukhaya Yelizovskaya	3	1	53.7	494	1 061
Sukhaya Yelizovskaya	4	3	14.2 ± 7.2	86	324
Tarfala	5	4	26.6 ± 10	316	815
Tsanyk	6	5	11.1 ± 6.9	221	1 141
Langery	7	32	51.5 ± 40	99	1 124
Dzhankuat	8	39	16.5 ± 11.5	1 184	3 141
Sukhoy Ilchinets	9	9	51.5 ± 45.5	2 123	3 091
Velesa	10	16	255 ± 171	8	85
Tarfala	11	8	28.5 ± 12.5	138	832
Tarfala	12	4	20.5 ± 3.5	12	194

[1] according to Table 1

For each hydrological event, the contribution of turbidity fluctuations within one hour was evaluated using the method described below.

Each hour, the difference between the maximum and minimum turbidity for a given period of time (ΔT_i) was calculated and referred to the difference in turbidity for the hydrological event (ΔT_{HE}):

$$\Delta T_i = T_{max} - T_{min} \qquad (1)$$

where T_{max}, T_{min} are the maximum and minimum turbidity values for the i period of time, NTU. The authors proposed to indicate the ratio of the range of variations of ΔT_i to ΔT_{HE} as T_I (turbidity index):

$$TI_{HE} = \frac{\Delta T_i}{\Delta T_{HE}} \qquad (2)$$

Thus, the calculation of the coefficient characterizing the mean contribution of urgent turbidity fluctuations for the entire series of observations was carried out using the following formula:

$$TI_{AV} = \frac{\sum_{i=1}^{n} TI_{HE}}{n}, \qquad (3)$$

where TI_{HE} is the index of optical turbidity fluctuations for a hydrological event, dimensionless; TI_{AV} is the index of fluctuations of optical turbidity for the whole series of observations, dimensionless; n is the number of hydrological events. An example of calculations for the Dzhankuat river is provided in Fig. 2.
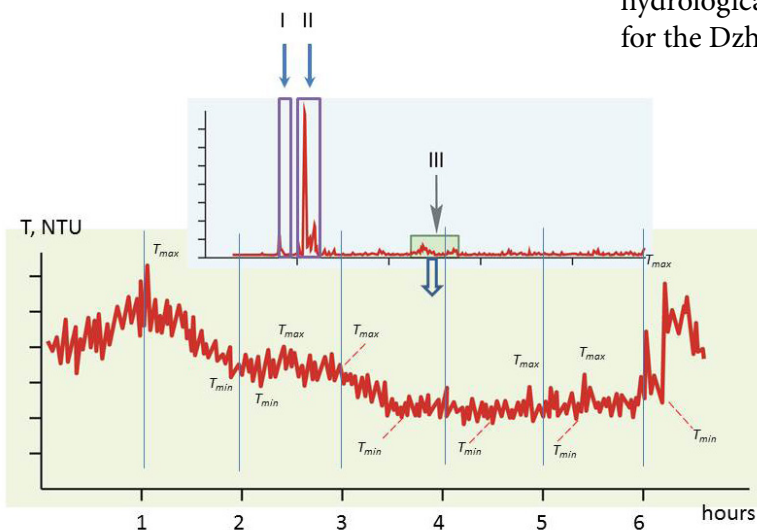
Figure 2. Method of sedigraph separation (I, II, III – hydrological events (HE)). An example of the breakdown into hydrological events and the calculation of the TI index for the Dzhankuat river (8th station).

3. Results and discussion

With the exception of the data recorded in 2017 by the SEBA logger at the Tarfala 12th station (see Table 1 for station numbers), the rivers with the glacial basin definitely form groups (the Tarfala, the Dzhankuat rivers), for which TI_{AV} is 0.17-0.22, the rivers in volcanic areas (the Sukhaya Yelizovskaya, the Sukhoy Ilchinets rivers), for which TI_{AV} is 0.22-0.25 and the lowland Selenga and Velesa rivers ($TI_{AV} = 0.09$). Average values of TI_{AV} coefficients are given in Table 3.

Table 3. Morphometric characteristics of river basins and characteristic values of TIAV coefficient

River	Station code[1]	F, km²	H_{AV}, m a.s.l.	L_{bas}, km	L, km	TI_{AV}	SD
Khaara	1	14 534	1 185	208	350	0.20	0.20
Selenga	2	440 000	600	800	897	0.09	0.07
Sukhaya Yelizovskaya	3	2	1 256	9	1	0.25	0.18
Sukhaya Yelizovskaya	4	1	1 441	2	2	0.22	0.18
Tarfala	5	21	1 430	6	2	0.17	0.14
Tsanyk	6	2	387	2	1	0.19	0.19
Langery	7	351	470	20	26	0.22	0.10
Dzhankuat	8	9	3 272	4	1	0.22	0.21
Sukhoy Ilchinets	9	135	523	24	27	0.22	0.24
Velesa	10	470	223	45	87	0.09	0.11
Tarfala	11	29	1 352	9	5	0.17	0.12
Tarfala	12	1	1 623	3	1	0.30	0.21

[1] according to Table 1

The maximum coefficients were determined in the rivers flowing in periglacial conditions (the Dzhankuat and the Tarfala), where the water runoff is formed due to ice and snow melting on the glacier, snow melting on the non-glacial part of the river basin, atmospheric precipitation and underground water (Vasylchuk et al., 2016). The variety of sources and the nature of their interactions in many ways predetermined such frequent short-term turbidity fluctuations (Stott and Grove, 2001) which drains a 560 km² partly glacierized catchment in north- east Greenland, is dominated by diurnal oscillations reflecting variations in the melt rate of snow and ice in the basin. Superimposed on this diurnal pattern are numerous short-lived discharge fluctuations of irregular periodicity and magnitude. The larger fluctuations are described and attributed to both rainfall events and periodic collapse of the glacier margin damming flow from beneath the Skelbrae glacier. Other minor fluctuations are less readily explained but are associated with changes in the channelized and distributed reservoirs and possibly temporary blockage of subglacial conduits caused by ice melt with subsequent damming. Fluctuations in suspended sediment concentration (SSC).

High turbidity fluctuations in the volcanic rivers are associated with their hydrological regime, characterized by short-term fluctuations in the water level due to the phenomenon of interaction between the channel and subsoil runoff (Chalov and Tsyplenkov, 2017; Chalov et al., 2017) headwater catchments located on volcanic slopes and valleys are characterized by distinctive hydrology and sediment transport patterns. However, lack of sufficient monitoring causes that the governing processes and patterns in these areas are rarely well understood. In this study, spatiotemporal water discharge and sediment transport from upstream sources was investigated in one of the numerous headwater catchments located in the lahar valleys of the Kamchatka Peninsula Sukhaya Elizovskaya River near Avachinskii and Koryakskii volcanoes. Three different subcatchments and corresponding channel types (wandering rivers within lahar valleys, mountain rivers within

volcanic slopes and rivers within submountain terrains.

A fairly large coefficient of the Tsanyk river is associated with the frequency and the nature of the diurnal turbidity peaks. Since the river flows in the zone of humid subtropics, the role of basin erosion (Golosov et al., 2012; Tsyplenkov et al., 2017) and, as a consequence, of rainfall intensity in the occurrence of turbidity fluctuations is extremely important. Due to very small basin areas (≈ 1 km^2), the material is quickly supplied to the river.

The relation of $TI_{AV} = f(F)$ is clearly negative, where F is the basin area expressed in km^2 (Fig. 3). And for very small rivers, with a basin area of less than 100 km^2, this relation has a high correlation coefficient $r = -0.7$. While for all rivers this relation is weaker ($r = -0.56$). There is certainly a relation with other morphometric characteristics of the basin area, but it is slightly weaker. Table 4 shows Pearson correlation r-coefficients of TI_{AV} and the basin area (F, km^2), the average altitude of the basin area (H_{AV}, m a.s.l.), the basin length (L_{bas}, km) and the river length (L, km).
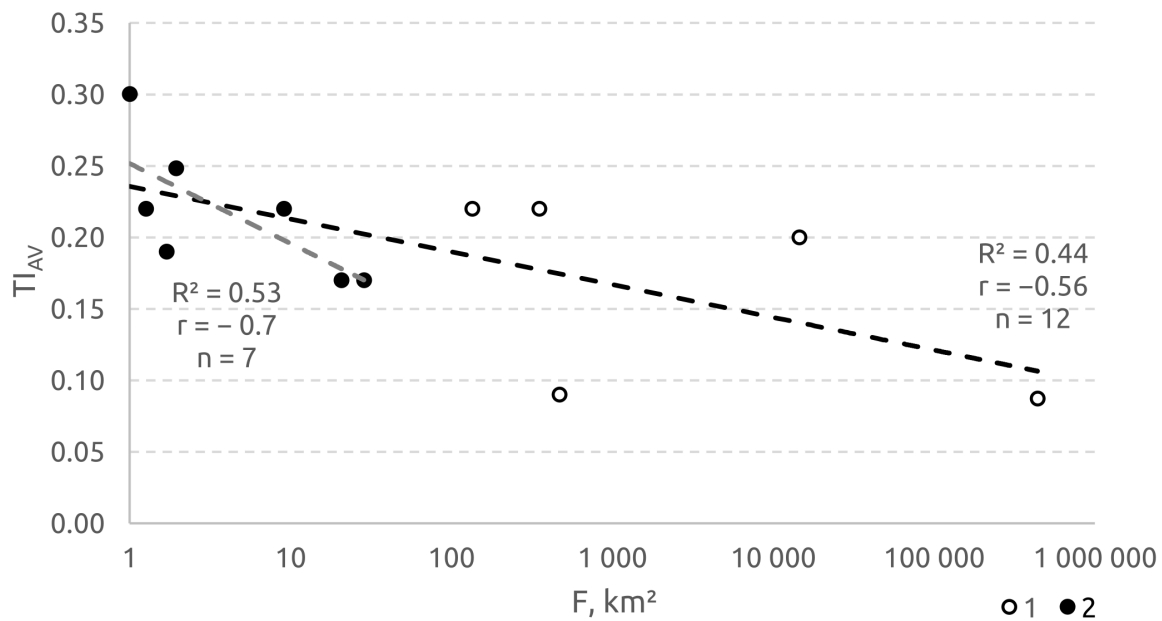
Figure 3. Relationship between TIAV and the basin area F (axis of abscissas is logarithmic): 1 – all rivers; 2 – small rivers (F < 100 km2).

**Table 4.** Pearson's correlation coefficients r of TAV and morphometric characteristics of the water basin area.

	F, km^2	H$_{AV}$, km	L$_{bas}$, km	L, km
Small (F < 100 km^2)	−0.70	0.20	−0.24	−0.66
All	−0.56	0.42	−0.57	−0.58

The analysis of the sets of observations revealed an inverse relationship between the TI_{HE} index and the duration of the hydrological event (Δt, hours). For the entire field of points, the r correlation coefficient is −0.42. However, when calculating the correlation for individual rivers (see Fig. 4), the average coefficient is −0.62.

Thus, the role of short-term turbidity fluctuations increases with the decrease in the

duration of river floods. The highest TI_{HE} was observed in the Dzhankuat and the Tsanyk during the rainfall flood (19.07.2016 and 10.04.2015), lasting for 4-6 hours. The lowest coefficients are characteristic of the low-flow periods on lowland rivers (the Velesa), where turbidity fluctuations for about 400 hours were 10 NTU ($TI_{HE} = 0.02$).

The origin of the trend in the relationship between the TI_{AV} index and the morphomet-
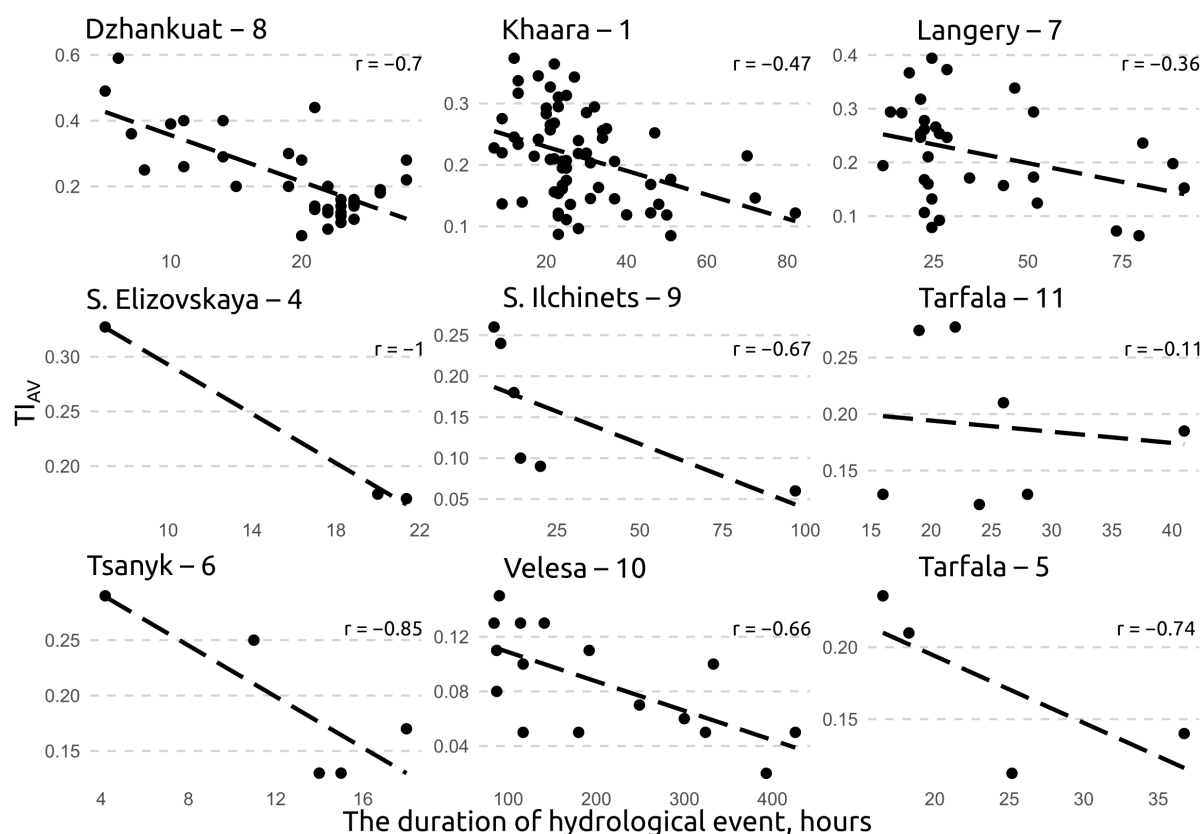
Figure 4. Relationship between the TI_{HE} coefficient and the duration of the hydrological event. Stations' codes according to Table 1.

ric characteristics of the basin area (*F*) can be indicative of the contribution of short-term fluctuations to the total sediment yield. Given the fact that the relationship with the average altitude (H_{AV}) of the basin area is positive, and with the basin area – negative, a significant part of the suspended sediment yield of the upper links of the river network is formed in very short time intervals (within a few hours).

4. Conclusions

The highest amplitudes of the diurnal turbidity and flow rates of the suspended sediments have been observed in small streams that are characterized by the highest channel slopes, relatively high transport capacity and small distances from sediment sources and rivers. The increase in the catchment area is associated with decreasing diurnal turbidity fluctuations. The observed pulses on the lowland rivers can be explained by the heterogeneity of sediment movement, and in particular by the constant mass transfer between different layers of water flow, bedload sediments, and bottom deposits.

Acknowledgements

References

Alekseevsky N.I., Belozerova E.V., Kasimov N.S., Chalov S.R. 2013. Prostranstvennaya izmenchivost kharakteristik stoka vzveshennykh nanosov v basseyne Selengu v period dozhdevykh pavodkov. Vestnik Moskovskogo Universiteta. Seria 5 Geografia 6(3), 60-65.

Belozerova E.V., Chalov S.R., 2013. Opredelenie mutnosti rechnykh vod opticheskimi metodami. Vestnik Moskovskogo Universiteta. Seria 5 Geografia 6(5), 39-45.

Chalov S.R., Tsyplenkov A.S., 2017. Stok nanosov malykh rek rayonov sovremennogo vulkanizma (r. Sukhaya Yelizovskaya, Kachatka). Geomorfologia 6(1), 104-116.

Chalov S.R, Tsyplenkov A.S, Pietron J., Chalova A.S., Shkolny D.I, Jahsjo J., Maerker M., 2017. Sediment transport in headwaters of a volcanic catchment—Kamchatka Peninsula case study. Front. Earth Sci. Frontiers of Earth Science 11(3), 565-578.

Clifford N.J., Richards K.S., Brown R.A., Lane S.N 1995. Scales of Variation of Suspended Sediment Concentration and Turbidity in a Glacial Meltwater Stream. Geogr. Ann. Ser. A, Phys. Geogr. 77(1-2), 45-65.

Gippel C.J., 1995. Potential of turbidity monitoring for measuring the transport of suspended solids in streams. Hydrol. Process. 9(1), 83-97.

Golosov V.N. Dela Seta M., Azhigirov A.A., Kuznetsova Y.S., Del' Monte M., Fredi P., Lupiya Pal'miyeri Ye., Grigor'yeva T.M 2012. Vlianie antropogennoy deyatelnosti na intensivnost ekzogennykh protsessov v nizkogoryakh subtropicheskogo poyasa. Geomorfologiya 2, 7-17.

Gray J.R., Gartner J.W., 2009. Technological advances in suspended-sediment surrogate monitoring. Water Resour. Res. 45(4), W00D29.

Horowitz A.J. 1990. Variations in suspended sediment and associated trace element concentrations in selected riverine cross sections. Environ. Sci. Technol. 24(9) 1313-1320.

Karaushev A.V., 1977. Teoriya i metody rascheta rechnykh nanosov. Gidrometeoizdat.

Karaushev A.V. Ed., 1977. Stok nanosov, ego izuchenie i geograficheskoye raspredelenie. Gidrometeoizdat.

Lewis J., 1996. Turbidity-Controlled Suspended Sediment Sampling for Runoff-Event Load Estimation. Water Resour. Res. 32(7), 2299-2310.

Polyakov B.V., 1946. Gidrologicheskiy analiz i raschety: Uchebnoye posobiye. Gydrometeoizdat.

Sloto R.A., Crouse M.Y., 1996. Hysep: a computer program for streamflow hydrograph separation and analysis. U.S. Geological Survey.

Stott T.A., Grove J.R., 2001. Short-term discharge and suspended sediment fluctuations in the proglacial Skeldal River, north-east Greenland. Hydrol. Process. 15(3), 407-423.

Stott T.A., Mount N.J., 2007a. The impact of rainstorms on short-term spatial and temporal patterns of suspended sediment transfer over a proglacial zone, Ecrins National Park, France. Effects of River Sediments and Channel Processes on Social, Economic and Environmental Safety, Proceedings of the Tenth International Symposium on River Sedimentation, Moscow, 259-266.

Stott T., Mount N., 2007b. Alpine proglacial suspended sediment dynamics in warm and cool ablation seasons: Implications for global warming. J. Hydrol. 332(3–4): 259-270.

Tsyplenkov A.S., Golosov V.N., Kuksina L.V., 2017. Otsenka basseynovoy sostavlyayuschey stoka vzveshennykh nanosov v malykh rechnykh basseynakh sukhikh i vlazhnykh subtropikov pri ekstremalnom stoke. Inzhenernye Izyskaniya 96, 54-65.

Walling D.E., 1977. Assessing the accuracy of suspended sediment rating curves for a small basin. Water Resour. Res. 13(3), 531-538.

Vasilchuk Y.K. Retz E.P., Chizhova Y.N., Tokarev I.V., Frolova N.L., Budantzeva N.A., Kireeva M.B, Loshakova N.A.. 2016. Raschleneniye gidrografa reki Dzhankuat, Tsentralnyi Kavkaz, s pomoschyu izotopnykh metodov. Vodnye resursy i rezhym vodnykh obyektov. 2016. 43(6), 579-594.